European Journal of Forest Research (2024) 143:581–601
https://doi.org/10.1007/s10342-023-01640-2

ORIGINAL PAPER

Evaluation of afforestations for avalanche protection with orthoimages using the random forest algorithm

Tina Grätz[1] · Sonja Vospernik[1] · Christian Scheidl[2]

Received: 25 April 2023 / Revised: 6 November 2023 / Accepted: 20 November 2023 / Published online: 4 January 2024

Abstract
Afforestations provide cost-effective and environmentally friendly protection against natural hazards, compared to technical measures. In Austria, more than 3000 afforestation sites for hazard protection covering 9000 ha have been established between 1906 and 2017, mainly for snow avalanche protection. The actual protective effect depends on avalanche predisposing factors and land cover, i.e. whether forest is present. In this study, predisposing factors and land cover classes were identified and analysed in selected afforestation sites. The protective effect of forest was attributed to the presence of forest cover and tree species. Using RGB images with a ground resolution of 20 × 20 cm, nine land cover categories have been distinguished by means of supervised classification with the random forest algorithm. Those land cover categories were classified with an overall accuracy of 0.87–0.98 and Kappa-values, ranging between 0.81 and 0.93. Images were filtered using a 3 pixel by 3 pixel majority filter, which assigns each cell in the output grid the most commonly occurring value in a moving window centred on each grid cell. This filter further increased the overall accuracy by removing noise pixels while preserving the fine elements of the classified grid. Our results indicate a protective effect for about half of the analysed afforestation sites. The dominance of the land use class "Meadow" at most sites with little avalanche protection effect suggests grazing as a limiting factor. The spatial information provided with the described method allows to identify critical areas in terms of avalanche protection even years after the initial afforestation.

Keywords High elevation afforestation · Random forest model · Protective forest · Avalanche protection · Remote sensing data · Aerial images

Introduction

In alpine regions, the protective function of forests is an important ecosystem service—reducing the risk of natural hazards like snow avalanches, rockfall, landslides or torrential floodings on humans and infrastructural facilities (Freudenschuss et al. 2021; Poratelli et al. 2020; Scheidl et al. 2020a, b; Sebald et al. 2019; Teich et al. 2019) and forests reduce runoff because of increased rainfall interception and increased transpiration during dry periods (e.g.: Andréassian 2004). In Austria, such forests, typically referred to as protective forests (Makino and Rudolf-Miklau 2021), have a share of 20.5%, and in the province of Tyrol they nowadays even have a share of around 50% (Amt der Tiroler Landesregierung, Gruppe Forst 2020). This is partly due to extensive reforestation projects at higher elevations, since the late 1960's (WIFO 1963) aiming at either supplementing or even substituting technical avalanche mitigation structures within avalanche release zones (Senn and Schönenberger 2001; Heumader 2000). Afforestations for hazard protection are thought to have a better cost–benefit ratio compared to solely technical protection measures (Mößmer 1998) and lower environmental impacts as well as higher adaption capacities to changing conditions (Albert et al. 2017; Nesshöver et al. 2017; Gasperl 2014). In Austria, more than 3000 afforestation sites have been established till today, covering about 9000 ha (Scheidl et al. 2021).

Communicated by Martin Ehbrecht.

✉ Sonja Vospernik
sonja.vospernik@boku.ac.at

1 Institute of Forest Growth, University of Natural Resources and Life Sciences, Peter Jordan Straße, 82 1190 Vienna, Austria

2 Institute of Mountain Risk Engineering, University of Natural Resources and Life Sciences, Peter Jordan Straße, 82 1190 Vienna, Austria

Afforestations for hazard protection were, however, not always successful, even though they were installed under consideration of the wind-snow-ecogram ("Wind-Schnee-Ökogramm") introduced by Aulitzky (1963). The wind-snow-ecogram takes microclimatic conditions into account by observing herbaceous species indicating wind-blown sites and sites with a very long snow cover duration; if such indicator plants are observed in the field, no trees are planted on the respective sites; thus, trees are only reforested on the climatically most favourable sites, easily recognisable by the ground vegetation. This is because regeneration at the timberline is exposed to extreme conditions and survival rates for tree growth at high altitudes are low because of harsh environmental conditions (Çolak 2003). Low temperatures, a short photoperiod, limited nutrient uptake from raw humus, snow bending, frost desiccation and pests (e.g. snow mould) become limiting for tree establishment (Körner 2012; Çolak 2003; Heikkinen et al. 2002).

The success of afforestations for hazard protection in Austria, however, has not been evaluated at a larger scale and it has not been tested if they fulfil the protective function, other than by regional site visits. This is because the number of afforestation sites is large, they are situated in remote areas and field assessment of all afforestations is therefore not cost-efficient. About 520 of these afforestation sites are also thought to have transitioned from the initial stage to a young stage raising the question of silvicultural management strategies such as precommercial thinning and thinning that maintain an acceptable level of protection by preserving tree and stand stability (Scheidl et al. 2021) and only few systematic studies have investigated silvicultural adaption strategies for "advanced" reforestations.

The factors determining the protective effect of a forest to minimise the risk of triggering avalanches are reasonably well known (Bebi et al. 2009). First, avalanches are only released in areas, that have a basic disposition for triggering events. The disposition for avalanches depends on slope, plan curvature and ruggedness (Bühler et al. 2013). Second, the forest has a mitigating effect on avalanche release by increasing the stability of the snowpack due to anchoring effects of trees, by interrupting the continuity of weak snow layers through snow interception from the canopy and by providing more favourable radiation and temperature conditions of the snow surface (Sykes et al. 2022). Thus, the protective capacity of mountain forests is generally assessed by the size and distribution of forest gaps, tree density and crown closure (Teich et al. 2012).

Disposing factors and forest parameters can be assessed using digital elevation models and remote sensing data. Multisource remote sensing data (Landsat satellite multispectral data, hyperspectral airborne data, radar data and geographic data) have been widely applied in the automatic detection of forest parameters (Fassnacht et al. 2016), in particular for the detection of tree species (Onishi and Ise 2021; Fassnacht et al. 2017; Immitzer et al. 2016; Waser et al. 2011), but rarely used for the evaluation of afforestations for hazard protection (Bebi et al. 2022, 2001; Breschan et al. 2018) or integrated in a consistent framework to assess the protective function against natural hazards. The reasons hampering such applications are manifold. Afforestations for hazard protection represent non-adjacent areas scattered across the landscape, so that the spectral composition of images differs between afforestation areas. Therefore, the type of background signal also varies with location and tree species density (Fassnacht et al. 2016). Finally, afforestations for hazard protection should be assessed in an early stage 5–10 years after planting to diagnose regeneration failure and take counter measures or to plan subsequent silvicultural treatment and the small tree size (e.g. expected crown diameter for a 10-m high Norway spruce tree is 3.1 m, (Kahn and Pretzsch 1998)) requires a high spatial resolution, excluding numerous sensors.

Nevertheless, remote sensing techniques seem to be particularly promising for surveys of high elevation afforested areas, because of the steep, inaccessible terrain. In recent years, the automatic detection of forest parameters from remote sensing data has been successively improved and has already been applied in numerous forestry issues. Tree species classification has been done with all types of sensors and at the individual tree or forest management level, but largescale applications are still rare (Fassnacht et al. 2016). Finally, RGB-images are freely available at high spatial resolution for all areas in Austria.

The intention of this study is to demonstrate a robust methodology to survey current land cover conditions of selected high elevation afforestation sites, whose protection purpose is to prevent avalanches from being triggered. The method is then further used to investigate how the land cover has changed compared to the initial state, which tree species dominate the afforested area today and how the land cover behaves regarding the requirements for protection against avalanche release.

In detail we aimed to answer the following questions:

- Can trees in afforestations for hazard protection be detected with sufficient accuracy using widely available RGB images to be able to evaluate afforestation success?
- Can protective land cover be modelled with an approach allowing large scale application?

Data and methods

Study site

The data for this study are based on information of 12 afforestation sites in the Paznaun and Stanzer Valley, Tyrol, Austria (Fig. 1), installed by the Forest Technical

Service of Avalanche and Torrent Control in Austria. Both valleys are located in West-Tyrol (Austria), covering montane to high-subalpine altitudes.

The climate is characterised by a continental mountain climate with pronounced summer precipitation. For both valleys, the annual average temperature is about 1.3 °C, the annual average precipitation amounts to 1109 mm, and the snow cover duration (more than 20 cm) lasts 193 days per year. The geology is dominated by gneiss with a high proportion of base-rich silicates and podzols or semi-podzols as soil types (Kilian et al. 1994). Afforestation campaigns were carried out between 1954 and 2014 at an altitude between 1220 and 2310 m above sea level.

In total, ten afforestation sites in the Paznaun Valley (#1–10, Table 1)—ranging from 1.2 to 75.4 ha—and two afforestation sites in the Stanzer Valley (#11–12, Table 1)—with 4.4 and 86.4 ha—were considered. These afforestations were randomly chosen from the 30 afforestation sites established in total in these two valleys. In all afforestation campaigns, the focus was on suitable tree species adapted to higher altitudes and the main tree species used were European larch (*Larix decidua* Mill.), Norway spruce (*Picea abies* L. (Karst.) and Swiss stone pine (*Pinus cembra* L.). Table 1 provides an overview of age, size, elevation and tree species initially afforested at the individual sites within the Paznaun and Stanzer Valley, respectively.

Avalanche disposition

The identification of possible avalanche release areas is based on slope, curvature and roughness and was determined by means of a digital elevation model with a resolution of 1 × 1 m (Amt der Tiroler Landesregierung, Tiris 2020) derived from airborne laser scanning data, which was acquired in 2018 for the southwest of Tyrol (Paznaun, afforestations 1–10) and in 2019 for the northwest of Tyrol (Stanzer Valley, afforestations 11–12). The slope thresholds for the potential release areas within the afforestation sites were 28°–60°. The roughness index reflects the degree of irregularity of the surface by highlighting the amount of elevation difference between adjacent cells of a digital elevation model. The plan curvature threshold was set to > 3 rad/100hm to eliminate highly convex or concave areas limiting the fracture propagation of avalanche release

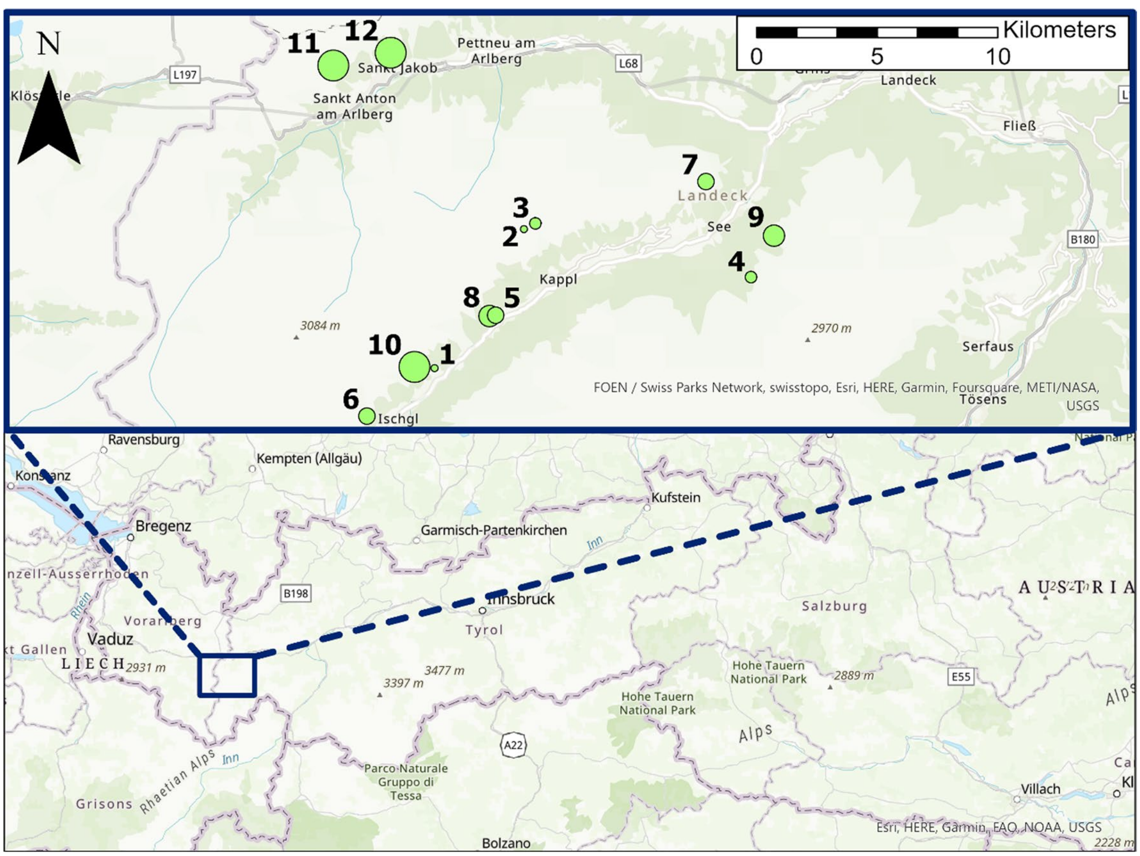

Fig. 1 Location of the study areas in the Paznaun and Stanzer Valley, Tyrol, Austria. The numbers correspond to the afforestation sites, and the size of the circles relates to the area afforested (c.f.: Table 1)

Table 1 Overview of the high elevation afforestations in the Paznaun and Stanzer Valley, Tyrol, Austria

#	Toponym	Year of afforestation	Max. age+ (years)	Area (ha)	Elevation (m a.s.l.)	Tree species
1	Ablenkdamm Platt	2003	18	2	1310–1510	PA, LD, PB
2	Diasbach	2005	16	9.5	2030–2180	PA, LD, PC, PU, AA, AV
3	Diasbach Damm	2008	13	1.9	2030–2060	PA, PC, PU, AV
4	Istalanzbach	1994	27	19.2	1960–2280	PA, LD, PC
5	Nederle	1990	31	1.8	1220–1290	PA, LD, SA
6	Paznauer Rinner	1955	66	1.6	1480–2040	PA, LD, PC
7	Schwager Gonde	1954	67	75.4	1380–2310	PA, LD, PC, SA, AP
8	Ulmicher	1999	22	1.2	1310–1380	PA, LD, SA, AP, PV
9	Versingalpe	2013	8	7.5	1960–2060	PA, LD, PC, PU
10	Vertschalrinnen	1992	29	2.7	1700–2080	PA, LD, PC
11	Kapall Fang	1983	38	4.4	1770–1930	PA, LD, PC
12	Putzenwald	1983	38	86.4	1300–1720	PA, LD, PS

PA Picea abies, Norway spruce, *LD Larix decidua*, European larch, *PC Pinus cembra*, Swiss stone pine, *PB Pinus strobus*, Eastern white pine, *PS Pinus sylvestris*, Scots pine, *PU Pinus uncinata*, mountain pine, *PM Pinus mugo*, Dwarf mountain pine, *AA Abies alba*, silver fir, *AV Alnus viridis*, green alder, *SA Sorbus aucuparia*, rowan, *AP Acer pseudoplatanus*, sycamore maple, *PV Prunus avium*, wild cherry

+Related to the year 2021

(Van Herwijnen et al. 2016). A threshold of 0.03 was used for rough terrain according to Bühler et al. (2018).

Land cover and tree species

For classification purpose, i.e. for the identification of the respective land cover categories per afforestation site, we applied a random forest model on red, green and blue spectral information of orthoimages acquired between 2015 – 2018 with a resolution 20 × 20 cm—provided by the Tyrolean spatial information system (Amt der Tiroler Landesregierung, Tiris 2020). Training pixels for each of the following 5 landcover classes were determined by visual delineation at all sites: (C1–C5) *Tree*, (C6) *Rock*, (C7) *Meadow*, (C8) *Shadow* and (C9) *Construction*. Subsequently, the category *Tree* was expanded to include a distinction of the specific tree species most frequently planted per afforestation area: (C1) Spruce (*Picea abies* L. (KARST.)), (C2) Larch (*Larix decidua* MILL.), (C3) Swiss stone pine (*Pinus cembra* L.), (C4) Evergreen and (C5) Hardwood. Norway spruce, European larch and Swiss stone pine are the tree species planted in almost all afforestations for hazard protection. Category C4 (*Evergreen*) includes other evergreen tree species, mainly Scots pine (*Pinus sylvestris* L.), Dwarf mountain pine (*Pinus mugo* subsp. *uncinata* (DC.) DOMIN) and *Engelmann spruce* (*Picea engelmannii* PARRY EX ENGELM.), which were, however, only present on few sites. The category C5 (*Hardwood*) includes all broadleaved trees (sycamore maple (*Acer pseudoplatanus* L.), silver birch (*Betula pendula* ROTH.*)*, ash (*Fraxinus excelsior* L.*)*, European aspen (*Populus tremula* L.*)*, rowan (*Sorbus aucuparia* L.*),* wild cherry (*Prunus avium* L.), green alder (*Alnus viridis* (CHAIX) DC.) and willow (*Salix spp.*)) as their protective effect against avalanches plays a rather minor role in the selected afforestation sites. Also, these species were often not planted but regenerated naturally at sites with lower elevation. For each category, at least 10 polygons per land cover type and at least 20 polygons per tree species were identified in each of the afforestation sites, when the respective category was present. Correct photointerpretation of tree species was verified by field survey. An overview of the final number of training plots compiled for each category and afforestation site is given in the Appendix (Table 5).

A random forest model estimating land cover class based on RGB-values of the orthoimages was trained for each site. The random forest algorithm trains an ensemble of decision trees, each decision tree classifies a pixel to a specific land cover class, and the final decision for a specific land cover class depends on the majority of votes from individual trees (Gislason et al. 2006). Of the several ensemble classification methods available, random forest uses an improved version of bagging (bootstrap aggregating). In bagging, a classifier is trained on bootstrapped samples from a training set, which has been shown to reduce the variance of the classification. Random forests have been shown to be comparable to boosting in terms of accuracies, but without the drawbacks of boosting (Breiman 2001).

Once classified, accuracy was assessed by a confusion matrix relating the number of automatically categorised pixels to referenced pixels, from which (i) the overall accuracy (p_o), (ii) the producer's accuracy (p_p), iii) the user's accuracy (p_u) and (iv) Cohens' Kappa (κ) could be derived.

The overall accuracy is calculated by dividing the number of correctly classified pixels (x_{cor}) of all categories by the total number of pixels (x_{tot}):

$$p_o = \frac{x_{cor}}{x_{tot}} \quad (1)$$

The producer's accuracy expresses if real features on the ground are correctly represented on the map. It is defined by the number of correctly classified pixels in each category (x_{cor}) divided by the total number of reference pixels (x_{ref}) for the considered category,

$$p_p = \frac{x_{cor}}{x_{ref}} \quad (2)$$

and represents map accuracy from the point of view of the map maker.

The user's accuracy expresses how often the class of the map will be present on the ground and is therefore also referred to as reliability. It is computed by dividing the number of correctly classified pixels in each category (x_{cor}) by the total number of pixels in that category (x_{cat}):

$$p_u = \frac{x_{cor}}{x_{cat}} \quad (3)$$

It represents the probability that a pixel classified into a given category actually represents that category on the ground.

The Kappa coefficient (Cohen 1960) evaluates how well the classification performed as compared to just randomly assigned values, i.e. did the classification do better than random. It can be calculated by relating the overall accuracy (p_o) with the probability of random agreement (p_e):

$$\kappa = \frac{p_o - p_e}{1 - p_e} \quad (4)$$

Thus, the lower the κ-value, i.e. the closer it gets to 0, the lower the random-adjusted agreement.

In a further step, the trained random forest model was applied to each afforestation site to model the spatial distribution of the pre-defined nine land cover categories (C1–C9). In the final step, predicted values were filtered with a majority filter. A majority filter assigns each cell in the output grid to the most commonly occurring value in a moving window centred on each grid cell. Neighbourhood size or filter size is determined by the user-defined x and y dimension. These dimensions should be odd, positive integer values. In this analysis a moving window of 3×3 pixels was chosen. Since the RGB-images have a resolution of 20 cm, the 3×3 pixel moving window corresponds to a 60 cm × 60 cm window on the ground. This small window size was selected to remove individual misclassified pixels, while preserving the information of small trees visible in the orthoimages and classified grids. The effective land cover area in terms of avalanche protection was then calculated by intersecting the modelled land cover classes with the avalanche disposition map.

Because the modelled tree-specific land cover categories do not comprise specific information on crown closure or tree density, and a detailed analyses of maximum gap width within the identified land cover results is out of the scope of this study, we assume the modelled tree specific land cover classes (C1, C2, C3, C4, C5) in relation to the total modelled non-forest areas (C6, C7, C9) as a first-order hazard assessment threshold. The class C8, shadow was omitted, since it could represent both a tree specific land cover class or non-forest area. Thus, in areas indicating potential avalanche triggering due to the disposition map, large tree land cover areas (i.e. protective areas) in relation to small non-forest areas suggest higher protection against the release of avalanches. Hence, a simple protective indicator in terms of avalanche protection is given by subtracting the share of non-forest areas from the share of protective areas. This performance indicator thus has a range from + 1 to − 1, depending on whether optimal or minimal to no protection is given. Vegetation height was calculated by subtracting the digital surface model (1 × 1 m resolution) from the digital terrain (1 × 1 m resolution) model using open government data (Amt der Tiroler Landesregierung, Tiris 2020). The resulting grids were used to visualize tree heights in the map of protective land cover.

Results

Classification accuracy and land cover prediction

The overall classification accuracy of the random forest model ranged between 0.87 and 0.98 and the Kappa-values ranged between 0.81 and 0.93. Overall, the random forest model showed relatively high producer (p_p) as well as user (p_u) accuracies for all land cover classes (Table 6). The detailed confusion matrices for each site are given in Appendix Tables 7–20.

The specific tree categories C1 Spruce, C2 Larch and C3 Swiss stone pine showed the greatest variance and mean producer's accuracies (Fig. 2 and Table 2). The reliability of C1 and C2, i.e. their users's accuracies, was in a similar range. The lowest user's accuracy was obtained for the land cover category C3 Swiss stone pine, which highlights the difficulty of its identification based on remote sensing data. The land use category in which evergreen tree species were grouped together (C4 Evergreen) shows overall lower variances and higher accuracy results, compared to the specific tree species categories C1–C3. The only broadleaved category, C5 Hardwood, includes so-called pioneer trees and is identified

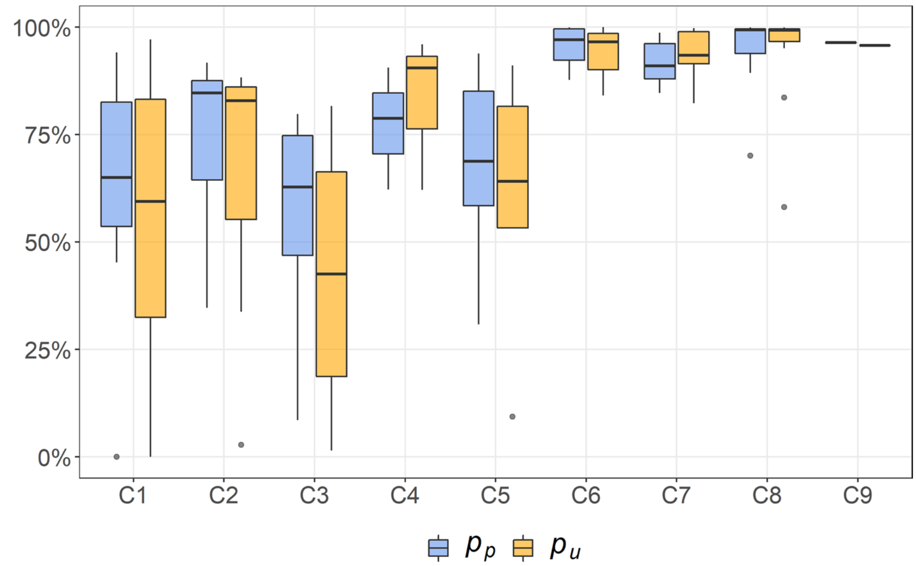

Fig. 2 Distributions of producer's (p_p) as well as user's (p_u) accuracies for each land-cover classification based on the results of the random forest model of all afforestation sites

Table 2 Percentage share of modelled land cover categories for each afforestation site

#	Toponym	Land cover share (%)								
		C1 Spruce	C2 Larch	C3 Swiss stone p	C4 Ever-green	C5 Hard-wood	C6 Rock	C7 Meadow	C8 Shadow	C9 Constr
1	Ablenkdamm Platt	4	25	0	0	**28**	12	18	13	0
2	Diasbach	0	2	11	17	1	2	**68**	0	0
3	Diasbach Damm	0	0	0	0	15	1	**83**	1	0
4	Istalanzbach	1	2	5	0	0	1	**81**	9	0
5	Nederle	**55**	8	0	0	8	0	4	25	0
6	Paznauer Rinner	**40**	5	0	0	0	4	6	45	0
7	Schwager Gonde	9	4	2	0	3	15	**45**	23	0
8	Ulmicher	**31**	8	0	0	19	0	16	26	0
9	Versingalpe	16	10	0	0	0	1	**35**	39	0
10	Vertschalrinnen	**38**	3	3	0	0	0	21	35	0
11	Kapall Fang	14	13	0	24	5	8	**25**	1	9
12	Putzenwald	16	0	0	10	0	1	**24**	49	0

The highest proportion, neglecting the land cover C8 shadow, is indicated by the bold representation

with similar accuracy by the random forest model as the category C1 Spruce. The highest producer and user accuracy values, however, result from the non-tree land cover categories C6 Rock, C7 Meadow and C8 Shadow, which can be identified nearly unambiguously. Because category C9 Construction is the least common land cover in the afforestation sites analysed here, its variability is non-existent and its accuracy high.

The percentage share of each category (C1–C9) per afforestation site (Table 2) indicates that most afforestation sites are either dominated by C1 Spruce or by C7 Meadows. Only for the deflecting dam (#1 Ablenkdamm Platt) Hardwood (C5) seems to prevail.

Land cover changes

For all afforestation plots investigated in this study, the number and species of trees planted are documented, which makes it possible to establish a baseline of tree species proportions per site. Compared to the proportion of tree species categories, identified by the random forest model, it is possible to assess a land cover change from the time of the last documented activity (plantation) until now. The change in tree specific land cover for each afforestation site is shown in Fig. 3, exclusively for tree specific land cover categories (C1–C5). In particular, at lower elevations the percentage of hardwoods increased over the years in relation to the afforestation (e.g. Ablenkdamm Platt, Ulmicher). Further over the

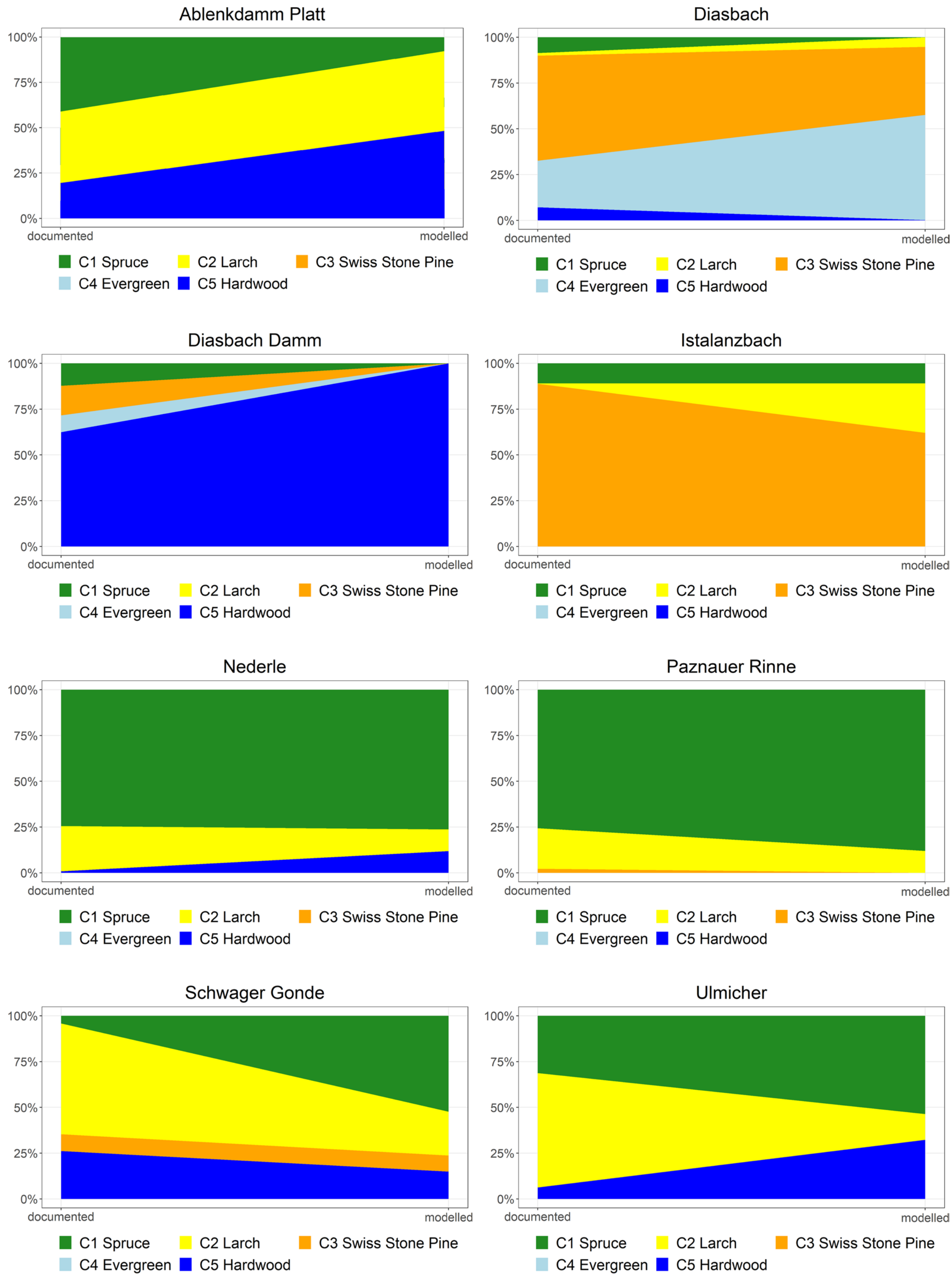

Fig. 3 Land cover changes from initial situation (as documented) to the most recent situation (modelled) for the tree specific categories C1–C5 within each afforestation site

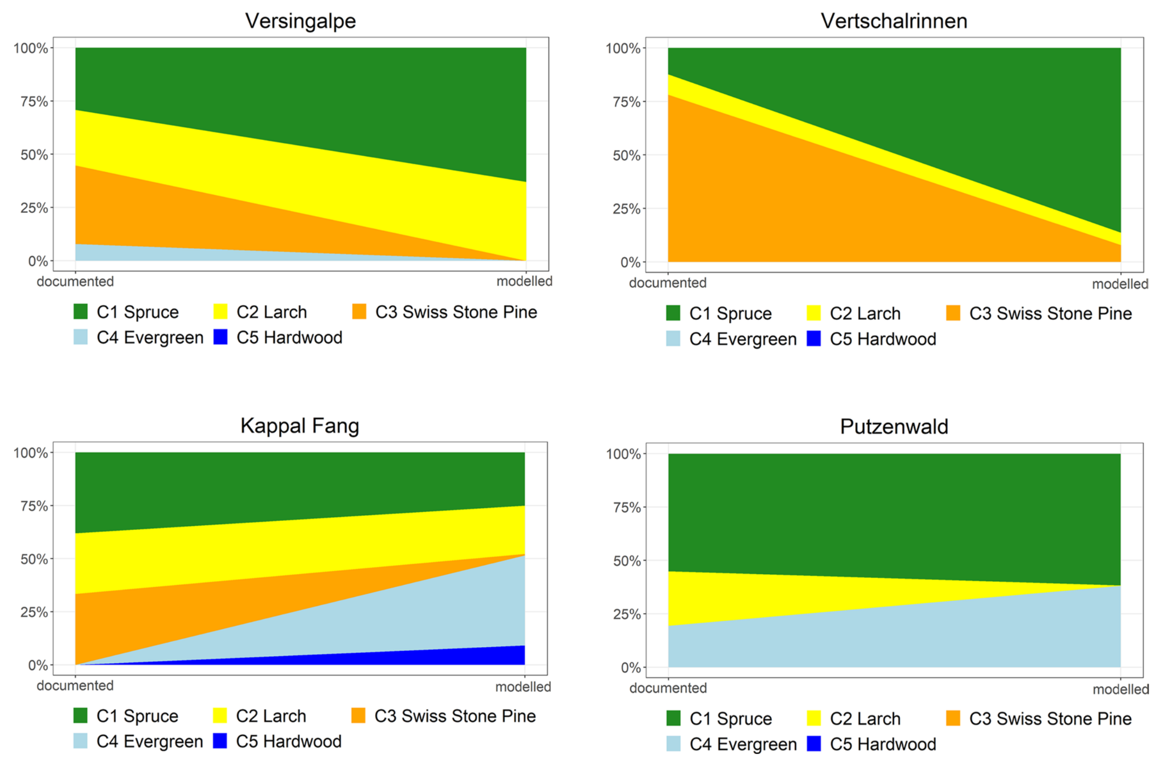

Fig. 3 (continued)

Table 3 Share of protective areas (all tree related land cover classes) and non-forested areas as a first assessment of the current protective effect of afforestation areas against avalanches

#	Toponym	Share of protective area (%)	Share of non-forest area+ (%)	Performance indicator (+1; −1]
1	Ablenkdamm Platt	59	26	0.33
2	Diasbach	32	68	−0.36
3	Diasbach Damm	17	83	−0.66
4	Istalanzbach	8	83	−0.75
5	Nederle	72	4	0.68
6	Paznauer Rinner	46	8	0.38
7	Schwager Gonde	18	59	−0.41
8	Ulmicher	58	16	0.42
9	Versingalpe	28	26	−0.02
10	Vertschalrinnen	47	15	0.32
11	Kapall Fang	57	43	0.14
12	Putzenwald	28	24	0.04

The results are based on the related shares of modelled land cover classifications intersected with the avalanche predisposition map

+not accounting for modelled land cover class C8 Shadow

years, Norway spruce seems to have outcompeted European larch and Swiss stone pine on some sites.

The highest share or protective area was found in study area 5 with 72% and the lowest share in study area 4 Istalanzbach. Accordingly, the performance indicator varied between −0.75 and 0.68 (Table 3).

Here, the performance indicator reflects to a certain extent the existing influence of non-forested areas, so-called potential gaps, in the artificial afforested avalanche release area. However, to minimise the risk of avalanches, knowledge of tree heights and their distribution is another important indicator in addition to knowledge of potential gaps. Table 4 lists the mean and standard deviation of tree heights > 1 m for tree specific land cover categories (C1–C5) of all afforestation sites analysed in this study.

An example of a comparison of the orthoimage of the afforestation site #1 Ablenkdamm with the modelled land cover classes is given in Fig. 4 (left and central panel). The right panel in Fig. 4 compares the avalanche disposition map with the spatial distribution of effective tree specific land cover categories as well as an indication of tree heights (c.f.: Table 4) and can be regarded as the current protective effect.

Further examples, comparing orthoimages of the recent land cover with modelled land cover classes and the final protected land cover predictions, are shown in the appendix (Fig. 5).

Table 4 Mean and standard deviation of tree heights for all trees > 1 m, listed by afforestation sites within modelled tree specific land cover categories (C1–C5)

#	Toponym	Distribution of tree heights > 1 m [m]				
		C1 Spruce	C2 Larch	C3 Swiss Stone P	C4 Evergreen	C5 Hardwood
1	Ablenkdamm Platt	4.8 ± 2.2	4.9 ± 2–2	–	–	4.8 ± 2.4
2	Diasbach	–	1.8 ± 1.1	1.3 ± 0.3	1.6 ± 0.8	2 ± 0.5
3	Diasbach Damm	–	–	–	–	1.2 ± 0.2
4	Istalanzbach	8.8 ± 6.6	9.9 ± 6.4	9.9 ± 6.0	–	–
5	Nederle	13.3 ± 3.2	15.7 ± 7.3	–	–	14.4 ± 4.6
6	Paznauer Rinner	18.8 ± 10.4	16.6 ± 9.3	6.9 ± 0	–	–
7	Schwager Gonde	15.5 ± 8.8	10.6 ± 7.4	9.4 ± 7.6	–	10.9 ± 7.2
8	Ulmicher	9.6 ± 5.1	8.1 ± 5.4	13.9 ± 6.9	–	–
9	Versingalpe	9.6 ± 6.2	10.8 ± 5.9	0 ± 0	0 ± 0	–
10	Vertschalrinnen	10.1 ± 6.5	4.5 ± 3.8	6.6 ± 7.9	–	–
11	Kapall Fang	2.2 ± 1.8	2.6 ± 1.5	1.8 ± 1.3	2.0 ± 1.2	2.1 ± 1.4
12	Putzenwald	17.4 ± 8.7	–	–	15.7 ± 8.0	–

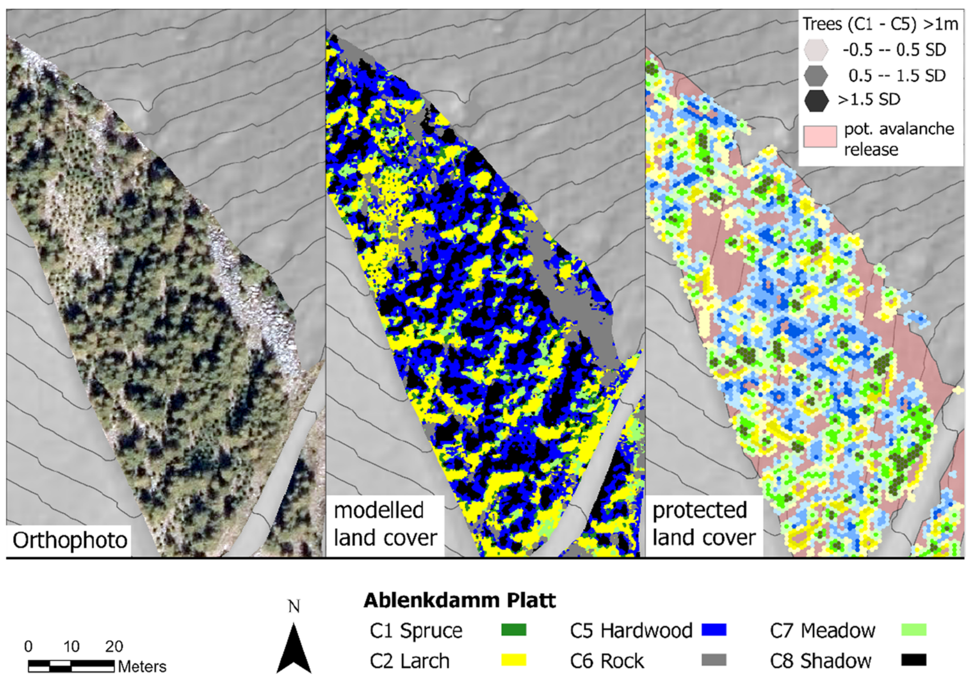

Fig. 4 Orthophoto (left) showing the real land cover situation, modelled land cover classifications based on the random forest model (centre) and intersection of avalanche release area (indicated in red) with the spatial distribution of effective tree specific land cover categories and tree heights(Table 4) (right) for the afforestation site 1: Ablenkdamm Platt

Discussion

Land cover and tree species classification

The quality of images used in this study was generally good with few shaded areas. Where shade prevailed, the respective area could not be assigned to a specific land cover class, which is an unsolvable problem if only orthoimages of one point in time are used (Waser et al. 2011). If images from different time points were available, or other auxiliary data were used, the classification might be improved in these areas. Where small, shaded areas were present, there was a transition zone between the sun-lit crown and the shaded area of the crown, which contained mixed pixels that were usually assigned to the shadow class decreasing the share of the trees; the tree class is therefore underrepresented leading to a slightly pessimistic assessment of the protective function. More generally, any land cover class overproportionally shaded would be underrepresented in the classification.

The study shows that land cover and tree species can be classified accurately from high-resolution RGB-images and classification accuracies attained were comparable or slightly better than those obtained in other land cover (Oduro Appiah et al. 2021; Talukdar et al. 2021; Toosi et al. 2019) or tree species classification studies using RGB (Eshetae 2020; Toscani 2012) or multispectral images (Immitzer et al. 2012). Meadow, shadow, rock or construction can be classified almost unambiguously, because there is little spectral overlap with the tree classes. Because of this, classification of the land cover classes is often very accurate, e.g. similar to a study by Lillesand et al. (2015). Similarly, the classification of tree species is very accurate on most sites, since the number of species to classify is low because only a limited number of tree species is able to grow at high elevation sites. Tree species classification results tend to be less accurate if more species are considered (Immitzer et al. 2012). Usually, classification is also poor when a low number of reference trees is available (Immitzer et al. 2012). This was, however, avoided in this study, by delineating an equal number of trees per species on orthoimages and measuring an equal number of trees per species as ground truth. The number of trees identified per species and afforestation corresponds to guidelines for training objects per class proposed by Lillesand et al. (2015), who suggest 10–100 training objects. Similarly, 10 polygons per land cover class were not found to be sufficient by Ma et al. (2017), but by increasing the number of polygons to 30 a good classification accuracy could be achieved in the study. In line with findings by Ma et al. (2017) other authors think that the selection of suitable training objects is more essential for high classification accuracies rather than an extremely large number of training polygons (Toscani 2012), so that the number of polygons used in this study can be considered sufficient and can be considered a reasonable effort, when a larger number of afforestations is to be evaluated.

The classification in this study was pixel-based. This type of classification is prone to individual misclassified noise-pixels (Immitzer et al. 2012). These could, however, be effectively removed by applying the 3 × 3 majority filter which increased overall accuracy and increased the users' and producers' accuracy for almost all sites and classes except for very small classes at some sites, where it decreased. In general, however, the 3 × 3 pixel filter preserved the signal from small size objects such as young trees in the regeneration or avalanche protectors.

The conifers except for larch were the classes most frequently misclassified, probably because of spectral overlap of these classes. In some afforestations, also Norway spruce, Scots pine and European larch or European larch and meadow were confused. In young afforestations, where lupins (*Lupinus angustifolius* L.) and rusty-leaved alpenrose (*Rhododendron ferrugineum* L.) were present, it was also not possible to distinguish these species from the trees, because of similar spectral bands and because they were intermingled with the crowns of the trees. Similar misclassification problems were also reported by Toscani (2012) and Rodriguez-Galiano et al. (2012). For the evaluation of the forest protection, however, only knowledge of the cover of evergreen conifers is required. So the misclassification between different evergreen tree species does not affect the evaluation of the protective function. Misclassifications with a consequence on the protective function are the confusion of evergreen trees with deciduous trees, which were, however, minor on most sites and the confusion of evergreen trees with mountain pine, which because of low height offers little protection against avalanches (Roloff et al. 2008). So further research should focus on distinguishing these classes.

With the nominal 20 cm ground resolution of the orthoimages, the resolution is generally good and available orthoimages were of good quality. In addition, the resolution of images increases with elevation since the flight height and distance from the terrain decrease resulting in smaller ground sampling distances for afforestations located at higher elevations; because of the good image quality even younger trees of the afforestations could be classified well although very small trees, with heights of less than 50–100 cm, were not visible in the images. Larger trees are, however, represented by numerous pixels. For example, a 10-m Norway spruce tree with an expected crown diameter of 3.1 m (estimate according to Kahn and Pretzsch (1998)) would be approximately represented by 38 pixels. Furthermore, the classification can be improved by using more data bands, auxiliary 3D-information from LIDAR data, or textural information (Immitzer et al. 2012). The simple classification is, however, accurate enough for the evaluation of the forest protection, since only the total cover of evergreen conifers is required.

The proportion of evergreen trees obtained from the orthoimages is expressed in canopy cover percent, which closely agrees with the canopy layer visible in remote sensing data and which is also the usual way of expressing species proportion in hazard protection frameworks (Perzl 2008; Frehner et al. 2005). This is because the protective function of the forest in terms of avalanche protection mostly depends on snow interception, which is closely related to canopy cover. In ground-based assessment species proportion is more often expressed in percent of stem number, basal area, volume or in relation to the maximum density of analysed tree species. This would be important, if economic use were prevalent, but less suitable for protection forests. Nevertheless, some guidelines refer to stem numbers because today terrestrial assessment is prevalent. In these cases, however, the guidelines could be adapted to contain canopy cover, since in protection forests canopy cover is the more meaningful variable.

First-order analyses of recent protective effects against avalanches

This study is the first to provide information on the protective performance against avalanches of afforestations in Austria, 8–66 years after their installation using automated image classification. A first step in the analysis of protective afforestations is the evaluation of the regeneration success (Heumader et al. 2017). At all sites trees planted could be successfully established, even though the initially planted tree species distribution changed considerably at some sites. The most notable changes are the natural establishment of hardwoods at lower elevations, and the increase in dominance of Norway spruce at most sites. Norway spruce seems to cope best with the site conditions typical for the Paznaun and Stanzer valley. Here, it has a competitive advantage over European larch, which is very light demanding (Ronch et al. 2016) and over Swiss stone pine, which is a slow growing species (Körner 2012). Swiss stone pine, however, dominates at sites close to the tree line, since it is better adapted to cold environments, being capable to photosynthesize at temperatures of 2–3 °C, whereas other conifers require a minimum temperature of 5 °C (Körner 2012). Swiss stone pine therefore forms the timberline in the study area.

In general, cover of tree species increases with time since establishment and the survival of planted trees depends on climatic and site-specific conditions (Körner 2012). Other important prerequisites for successful afforestations at the tree line are the use of suitable seed provenances and the consideration of suitable micro-sites of the local relief (Schönenberger et al. 1994; Sauermoser 1988). However, particularly older afforestation sites were often established with tree provenances that were not appropriate for the site conditions (Heumader 2000), which repeatedly led to major failures especially in temporal overlap with a cooling process that began around 1940 and lasted for several decades (Mayewski et al. 2004). Further, every irregularity in the slope surface causes extensive small-scale variation in the environmental conditions (Turner et al. 1983). This variation between microsites in addition with inappropriate tree provenances might also be reflected in the diverse performance indicators of the analysed afforestation sites in this study (Table 3). Factors limiting tree establishment in the Paznaun and Stanzer valley are low temperatures, a short photoperiod, limited nutrient uptake from raw humus, snow bending, frost desiccation and pests (e.g. snow mould) close to the tree line (Heikkinen et al. 2002; Çolak 2003; Körner 2012) and grazing and competing vegetation at lower elevation sites. Moreover, browsing by red deer (*Cervus elaphus* L.), roe deer (*Capreolus capreolus* L.) and chamoix (*Rupicapra rupricapra* L.) as well as fraying and bark stripping can limit tree establishment (e.g. Gerhard et al. 2013). Trees planted in the afforestations were, however, protected against game damage and when surveying sites game damage was not observed as major factor limiting tree establishment.

Conclusion

Summarising, land cover classification and hazard predisposition mapping are a cost-efficient way of evaluating a larger number of afforestations for hazard protection, in an objective manner. The land cover classification with the spectral bands red, green and blue can provide high classification accuracies, if the quality of orthoimages is good and if a sufficient number of training pixels is available. Large, shaded areas and spectral overlap pose the biggest problems in the land cover classification. Using additional information from other sensors might further improve the approach. The 3×3 majority filter effectively removes noise pixels, so that the method provides an effective way to evaluate afforestations for hazard protection.

The methodological frame-work proposed can be applied to large areas, since no field survey is required. Given the high number of sites afforested, this is an important advantage. Since orthoimages are acquired on a regular basis by the government of Tyrol also repeated classification and change detection of the afforestations is possible with this approach allowing monitoring of afforestations sites, which can give valuable insights for planning future afforestations and opens many opportunities for analysing the afforestation success scientifically. In case of regeneration failure, site visits to determine the environmental factors that inhibit regeneration at specific sites can further complement the approach. Afforestations for avalanche protection are environmentally friendly and cost-efficient, but a long time is needed for them to be fully efficient.

Appendix

See Tables 5, 6, 7, 8, 9, 10, 11, 12, 13, 14, 15, 16, 17, 18.

Table 5 Number of training plots for each category and afforestation site—identified by orthophotos from 2015 to 2018

#	C1	C2	C3	C4	C5	C6	C7	C8	C9
1	27	35	–	–	32	10	10	15	–
2	1	12	10	35	12	10	10	7	–
3	–	–	–	–	27	10	10	1	–
4	33	37	49	–	–	10	10	10	–
5	33	26	–	–	23	–	7	17	–
6	57	16	5	–	–	4	8	7	–
7	16	24	34	–	23	10	10	20	–
8	28	30	–	–	28	–	10	10	–
9	28	17	–	–	–	6	10	10	–
10	32	23	14	–	–	3	6	7	–
11	58	12	3	19	10	10	10	10	10
12	29	25	–	29	–	10	12	18	–

C1, Spruce; C2, Larch; C3, Swiss stone pine; C4, Evergreen; C5, Hardwood; C6, Rock; C7, Meadow; C8, Shadow; C9, Construction

Table 6 Mean and standard deviation of producer's and user's accuracies for each land cover category

Land cover categories	Producer's accuracy p_p (%)		User's accuracy p_p (%)	
	M	SD	*M*	SD
C1 Spruce	64	27	58	32
C2 Larch	75	20	68	28
C3 Swiss stone Pine	56	27	42	32
C4 Evergreen	77	14	83	18
C5 Hardwood	69	22	62	28
C6 Rock	96	4	94	6
C7 Meadow	92	5	93	5
C8 Shadow	95	9	94	12
C9 Construction	96	–	96	–

Table 7 Confusion matrix Ablenkdamm

Class	Predicted					
	C1	C2	C5	C6	C7	C8
Observed						
C1	1284	30	828	6	84	24
C2	12	9294	300	0	294	0
C5	24	24	15,882	0	744	30
C6	0	0	0	5574	0	0
C7	0	60	36	0	11,592	0
C8	0	0	126	0	0	21,156

C1 Spruce, *C2* Larch, *C3* Swiss stone pine, *C4* Evergreen, *C5* Hardwood, *C6* Rock, *C7* Meadow, *C8* Shadow, *C9* Construction

Table 8 Confusion matrix Diasbach

Class	Predicted						
	C2	C3	C4	C5	C6	C7	C8
Observed							
C1	8	0	776	0	0	0	0
C2	13,312	120	760	0	0	384	0
C3	408	3728	2240	0	0	1744	0
C4	160	456	63,056	8	0	808	0
C5	48	0	9968	1336	0	0	0
C6	0	0	8	0	17,496	104	0
C7	88	104	0	0	0	174,976	0
C8	0	0	168	0	0	0	4592

C1 Spruce, *C2* Larch, *C3* Swiss stone pine, *C4* Evergreen, *C5* Hardwood, *C6* Rock, *C7* Meadow, *C8* Shadow, *C9* Construction

Table 9 Confusion matrix Diasbach Damm

Class	Predicted			
	C5	C6	C7	C8
Observed				
C5	2428	0	408	0
C6	0	1596	0	0
C7	0	0	46,712	0
C8	32	0	0	108

C1 Spruce, *C2* Larch, *C3* Swiss stone pine, *C4* Evergreen, *C5* Hardwood, *C6* Rock, *C7* Meadow, *C8* Shadow, *C9* Construction

Table 10 Confusion matrix Istalanzbach

Class	Predicted					
	C1	C2	C3	C6	C7	C8
Observed						
C1	10,932	3480	15,318	0	5886	0
C2	900	48,540	4032	0	2646	0
C3	1938	690	62,142	12	3096	6
C6	0	12	36	5496	66	6
C7	552	666	2742	0	812,628	0
C8	0	0	0	0	6	139,098

C1 Spruce, *C2* Larch, *C3* Swiss stone pine, *C4* Evergreen, *C5* Hardwood, *C6* Rock, *C7* Meadow, *C8* Shadow, *C9* Construction

Table 11 Confusion matrix Nederle

Class	Predicted				
	C1	C2	C5	C7	C8
Observed					
C1	20,150	0	265	0	30
C2	510	30,970	690	1200	0
C5	1425	225	6520	65	5
C7	0	2670	280	26,245	0
C8	15	0	0	0	27,770

C1 Spruce, *C2* Larch, *C3* Swiss stone pine, *C4* Evergreen, *C5* Hardwood, *C6* Rock, *C7* Meadow, *C8* Shadow, *C9* Construction

Table 12 Confusion matrix Paznauer Rinner

Class	Predicted					
	C1	C2	C3	C6	C7	C8
Observed						
C1	50,538	600	0	0	24	0
C2	198	19,650	0	6	528	0
C3	2232	312	90	0	0	0
C6	0	0	0	4914	18	0
C7	126	498	0	30	14,232	0
C8	0	0	0	0	0	39,936

C1 Spruce, *C2* Larch, *C3* Swiss stone pine, *C4* Evergreen, *C5* Hardwood, *C6* Rock, *C7* Meadow, *C8* Shadow, *C9* Construction

Table 13 Confusion matrix Schwager Gonde

Class	Predicted						
	C1	C2	C3	C5	C6	C7	C8
Observed							
C1	6391	0	105	28	0	4928	91
C2	77	10,290	7	392	0	7805	7
C3	511	0	8239	21	0	1078	287
C5	203	896	0	8743	0	5257	49
C6	0	0	0	0	340,543	0	0
C7	84	154	21	182	0	449,260	0
C8	70	0	91	0	0	224	37,751

C1 Spruce, *C2* Larch, *C3* Swiss stone pine, *C4* Evergreen, *C5* Hardwood, *C6* Rock, *C7* Meadow, *C8* Shadow, *C9* Construction

Table 14 Confusion matrix Ulmicher

Class	Predicted				
	C1	C2	C5	C7	C8
Observed					
C1	12,185	0	1650	0	5
C2	5	6505	35	1615	0
C5	1510	200	36,900	275	0
C7	0	1045	215	28,155	0
C8	5	0	0	0	23,685

C1 Spruce, *C2* Larch, *C3* Swiss stone pine, *C4* Evergreen, *C5* Hardwood, *C6* Rock, *C7* Meadow, *C8* Shadow, *C9* Construction

Table 15 Confusion matrix Versingalpe

Class	Predicted				
	C1	C2	C6	C7	C8
Observed					
C1	17,270	820	0	4900	25
C2	1545	22,110	0	310	20
C6	10	0	4790	380	0
C7	1805	10	0	72,095	0
C8	0	0	0	5	27,520

C1 Spruce, *C2* Larch, *C3* Swiss stone pine, *C4* Evergreen, *C5* Hardwood, *C6* Rock, *C7* Meadow, *C8* Shadow, *C9* Construction

Table 16 Confusion matrix Vertschalrinnen

Class	Predicted					
	C1	C2	C3	C6	C7	C8
Observed						
C1	13,818	12	36	0	162	0
C2	54	5322	6	0	312	0
C3	12	0	780	0	84	0
C6	0	0	0	534	54	0
C7	168	0	0	0	16,770	0
C8	0	0	0	0	0	15,276

C1 Spruce, *C2* Larch, *C3* Swiss stone pine, *C4* Evergreen, *C5* Hardwood, *C6* Rock, *C7* Meadow, *C8* Shadow, *C9* Construction

Table 17 Confusion matrix Kapall Fang

Class	Predicted								
	C1	C2	C3	C4	C5	C6	C7	C8	C9
Observed									
C1	24,462	387	0	3519	558	0	18	0	0
C2	441	3555	0	252	180	0	252	0	0
C3	27	0	198	171	0	0	0	0	0
C4	756	0	0	50,724	0	0	0	0	0
C5	1566	108	0	27	11,799	0	333	0	0
C6	0	0	0	0	0	9387	0	0	0
C7	0	9	0	0	423	0	18,549	0	0
C8	0	0	0	0	0	0	0	22,482	0
C9	0	0	0	0	0	0	36	0	3438

C1 Spruce, *C2* Larch, *C3* Swiss stone pine, *C4* Evergreen, *C5* Hardwood, *C6* Rock, *C7* Meadow, *C8* Shadow, *C9* Construction

Table 18 Confusion matrix Putzenwald

Class	Predicted					
	C1	C2	C4	C6	C7	C8
Observed						
C1	19,260	0	2172	0	6636	54
C2	414	726	564	0	28,404	0
C4	2598	0	16,632	0	3408	66
C6	0	0	30	80,442	276	0
C7	2976	24	1980	114	499,572	26,346
C8	486	0	498	0	312	225,432

C1 Spruce, *C2* Larch, *C3* Swiss stone pine, *C4* Evergreen, *C5* Hardwood, *C6* Rock, *C7* Meadow, *C8* Shadow, *C9* Construction

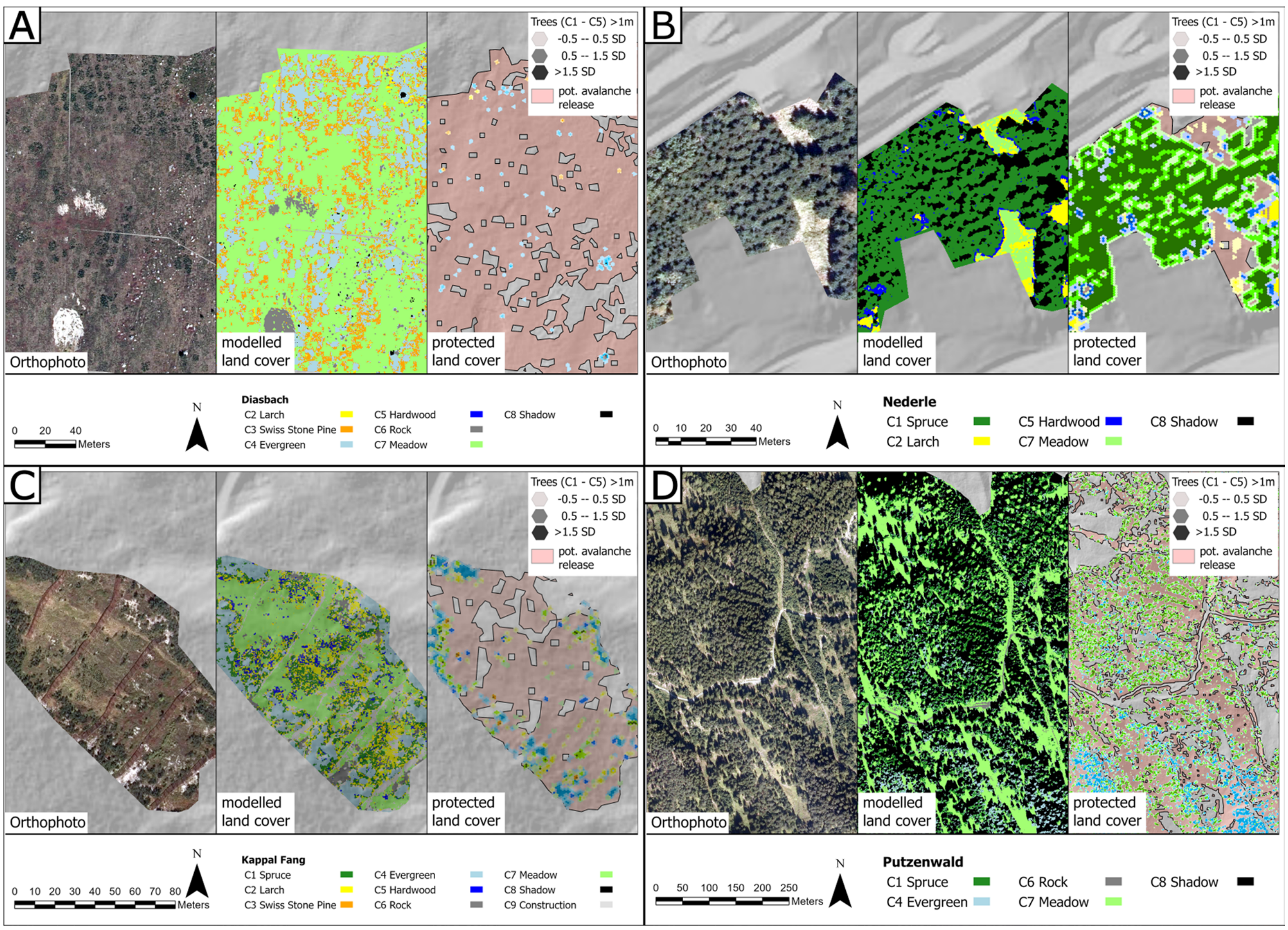

Fig. 5 Examples of afforestation sites **A** Diasbach, **B** Nederle, **C** Kapall Fang and **D** Putzenwald. For each example, the left pattern shows the real land cover situation (orthophoto), the pattern in the centre shows the modelled land cover classifications based on the random forest model, whereas the left pattern indicates recent avalanche protection effect of the related afforestation site by intersection of the basic avalanche release area (indicated in red) with the spatial distribution of effective tree specific land cover categories and tree heights (c.f.: Table 4)

Examples of afforestation sites (Fig. 5), comparing the real land cover situation (orthophoto, left pattern) with the results of the modelled land cover classification for each example (central pattern). Also shown is the current avalanche protective effect of the related afforestation site by intersection of the basic avalanche disposition map with the spatial distribution of effective tree specific land cover categories as well as an indication of recent tree heights (right pattern).

Author contributions TG, CS and SV* contributed to conceptualization, formal analysis, investigation, data curation, writing—original draft, writing review and editing, and visualization.

Funding Open access funding provided by University of Natural Resources and Life Sciences Vienna (BOKU).

Declarations

Conflict of interest The authors declare no conflict of interest.

References

Albert C, Spangenberg JH, Schröter B (2017) Nature-based solutions: criteria. Nature 543(7645):315. https://doi.org/10.1038/543315b

Andréassian V (2004) Waters and forests: from historical controversy to scientific debate. J Hydrol 291(1):1–27. https://doi.org/10.1016/j.jhydrol.2003.12.015

Aulitzky H (1963) Grundlagen und Anwendung des vorläufigen Wind-Schnee Ökogrammes (Mitteilungen der forstlichen Bundesversuchsanstalt Mariabrunn). In: Forstlichen Bundesversuchsanstalt Mariabrunn in Schönbrunn (eds), Ökologische Untersuchungen in der subalpinen Stufe zum Zwecke der Hochlagenaufforstung Teil 2. Österreichischer Agrarverlag, Wien

Bebi P, Kienast F, Schönenberger W (2001) Assessing structures in mountain forests as a basis for investigating the forests. Dynamics and protective function. For Ecol Manag 145(1–2):3–14

Bebi P, Kulakowski D, Rixen C (2009) Snow avalanche disturbances in forest ecosystems: state of research and implications for management (disturbances in mountain forests—implications for management). For Ecol Manage 257(9):1883–1892. https://doi.org/10.1016/j.foreco.2009.01.050

Bebi P, Bast A, Helzel K, Schmucki G, Brozova N, Bühler Y (2022) Avalanche protection forest: from process knowledge to interactive maps. In: Michaela Teich, Cristian Accastello, Frank Perzl, Karl Kleemayr (ed) Protective forests as ecosystem-based solution for disaster risk reduction (Eco-DRR). IntechOpen. https://doi.org/10.5772/intechopen.99514

Breiman L (2001) Random forests. Mach Learn 45(1):5–32. https://doi.org/10.1023/A:1010933404324

Breschan JR, Gabriel A, Frehner M (2018) A topography-informed morphology approach for automatic identification of forest gaps critical to the release of avalanches. Rem Sens 10(3):433. https://doi.org/10.3390/rs10030433

Bühler Y, Kumar S, Veitinger J, Christen M, Stoffel A, Snehmani (2013) Automated identification of potential snow avalanche release areas based on digital elevation models. Nat Hazards Earth Syst Sci 13(5):1321–1335. https://doi.org/10.5194/nhess-13-1321-2013

Bühler Y, von Rickenbach D, Stoffel A, Margreth S, Stoffel L, Christen M (2018) Automated snow avalanche release area delineation: validation of existing algorithms and proposition of a new object-based approach for large-scale hazard indication mapping. Nat Hazards Earth Syst Sci 18(12):3235–3251. https://doi.org/10.5194/nhess-18-3235-2018

Cohen J (1960) A coefficient of agreement for nominal scales. Educ Psychol Measur 20(1):37–46. https://doi.org/10.1177/001316446002000104

Çolak A (2003) Effects of microsite conditions on scots pine (*Pinus sylvestris* L.) seedlings in high-elevation plantings. Forstwiss Centbl 122(1):36–46. https://doi.org/10.1046/j.1439-0337.2003.t01-1-20431.x

Eshetae MA (2020) Tree species classification using UAV-RGB images and machine learning algorithms in a mixed temperate forest: a case study of Haagse Bos, Netherlands. Masterthesis. Enschede, Netherlands: University of Twente.

Fassnacht FE, Latifi H, Stereńczak K, Modzelewska A, Lefsky M, Waser LT, Straub C, Ghosh A (2016) Review of studies on tree species classification from remotely sensed data. RSE 186:64–87. https://doi.org/10.1016/j.rse.2016.08.013

Fassnacht FE, Mangold D, Schäfer J, Immitzer M, Kattenborn T, Koch B, Latifi H (2017) Estimating stand density, biomass and tree species from very high resolution stereo-imagery: towards an all-in-one sensor for forestry applications? Forestry 90(5):613–631. https://doi.org/10.1093/forestry/cpx014

Frehner M, Wasser B, Schwitter R (2005) Nachhaltigkeit und Erfolgskontrolle im Schutzwald. Wegleitung für Pflegemassnahmen in Wäldern mit Schutzfunktion, Vollzug Umwelt. Bundesamt für Umwelt, Wald und Landschaft, Bern. Zugriff am 30.9.2020. Verfügbar unter: https://www.bafu.admin.ch/bafu/de/home/themen/thema-wald-und-holz/wald-und-holz--publikationen/publikationen-wald---holz/nachhaltigkeit-und-erfolgskontrolle-im-schutzwald.html

Freudenschuss A, Markart G, Scheidl C, Schadauer K (eds.) (2021) Schutzwald in Österreich- Wissenstand und Forschungsbedarf. Kurzfassung. Bundesforschungszentrum für Wald, Wien

Gasperl W (2014) Schutzwald als Grundlage für den alpinen Lebensraum Naturgefahren und Schutzwald. BFW Praxisinform 34:12–14

Gerhard P, Arnold JM, Hackländer K, Hochbichler E (2013) Determinants of deer impact of European forest. a systematic literature analysis. For Ecol Manage 310:173–186

Gislason PO, Benediktsson JA, Sveinsson JR (2006) Random forests for land cover classification (pattern recognition in remote sensing (PRRS 2004)). Pattern Recognit Lett 27(4):294–300. https://doi.org/10.1016/j.patrec.2005.08.011

Heikkinen O, Tuovinen M, Autio J (2002) What determines the timberline? Fennia 180(1–2):67–74

Heumader J, Neuner J, Markart G (2017) Evaluierung von Hochlagenaufforstungen in Österreich. Schutzwald Waldwirkungen 180:232–239

Heumader J (2000) High-elevation afforestation and regeneration of subalpine forest stands eperiences in Austria. Interpreavent 2000 - Villach, Villach, Österreich, pp 29–40

Immitzer M, Atzberger C, Koukal T (2012) Tree species classification with random forest using very high spatial resolution 8-band worldview-2 satellite data. Rem Sens 4(9):2661–2693. https://doi.org/10.3390/rs4092661

Immitzer M, Vuolo F, Atzberger C (2016) First experience with sentinel-2 data for crop and tree species classifications in central Europe. Rem Sens 8(3):166. https://doi.org/10.3390/rs8030166

Kahn M, Pretzsch H (1998) Parametrisierung und Validierung des Wuchsmodells SILVA 2.2 für Rein- und Mischbestände aus Fichte, Tanne, Kiefer, Buche, Eiche und Erle. Kevelaer: Jahrestagung des Deutschen Verbands Forstlicher Forschungsanstalten vom 25.-27. Mai 1998

Kilian W, Müller F, Starlinger F (1994) Die forstlichen Wuchsgebiete Österreichs. No. 82. Forstliche Bundesversuchsanstalt

Körner C (2012) Alpine treelines: functional ecology of the global high elevation tree limits. Springer, Basel

Lillesand TM, Kiefer RW, Chipman JW (2015) Remote sensing and image interpretation, 7th edn. Wiley, Hoboken

Ma L, Li M, Ma X, Cheng L, Du P, Liu Y (2017) A review of supervised object-based land-cover image classification. ISPRS J Photogramm Rem Sens 130:277–293. https://doi.org/10.1016/j.isprsjprs.2017.06.001

Makino Y, Rudolf-Miklau F (2021) The protective functions of forests in a changing climate: European experience (Forestry working paper). FAO and Austrian Federal Ministry for Agriculture, Regions and Tourism

Mayewski PA, Rohling EE, Curt Stager J, Karlén W, Maasch KA, Meeker LD, Meyerson EA, Gasse F, van Kreveld S, Holmgren K, Lee-Thorp J, Rosqvist G, Rack F, Staubwasser M, Schneider RR, Steig EJ (2004) Holocene climate variability. Quat Res 62(3):243–255. https://doi.org/10.1016/j.yqres.2004.07.001

Mößmer EM (1998). Ohne Schutzwald geht's bergab! Intakte Bergwälder: lebensversicherung für das nächste Jahrtausend. Veröffentlichungen der Stiftung Wald in Not

Nesshöver C, Assmuth T, Irvine KN, Rusch GM, Waylen KA, Delbaere B, Haase D, Jones-Walters L, Keune H, Kovacs E, Krauze K, Külvik M, Rey F, van Dijk J, Vistad OI, Wilkinson ME, Wittmer H (2017) The science, policy and practice of nature-based solutions: an interdisciplinary perspective. Sci Total Environ 579:1215–1227. https://doi.org/10.1016/j.scitotenv.2016.11.106

Oduro Appiah J, Agyemang-Duah W, Sobeng AK, Kpienbaareh D (2021) Analysing patterns of forest cover change and related land uses in the Tano-Offin forest reserve in Ghana: implications for forest policy and land management. Trees For People 5:100105. https://doi.org/10.1016/j.tfp.2021.100105

Onishi M, Ise T (2021) Explainable identification and mapping of trees using UAV RGB image and deep learning. Sci Rep 11(1):903. https://doi.org/10.1038/s41598-020-79653-9

Perzl F (2008) Ein minimalstandard für die dokumentation der Schutzwirkungen des waldes im rahmen der österreichischen, Initiative Schutz durch Wald". INTERPRAEVENT 2008—conference proceedings. Villach, Österreich: Internationale Forschungsgesellschaft Interpraevent. pp 551–562

Poratelli F, Cocuccioni S, Accastello C, Steger S, Schneiderbauer S, Brun F (2020) State-of-the-art on ecosystem-based solutions for disaster risk reduction: the case of gravity-driven natural hazards in the Alpine region. Int J Disaster Risk Reduct 51:101929. https://doi.org/10.1016/j.ijdrr.2020.101929

Rodriguez-Galiano VF, Ghimire B, Rogan J, Chica-Olmo M, Rigol-Sanchez JP (2012) An assessment of the effectiveness of a random forest classifier for land-cover classification. ISPRS J Photogramm Rem Sens 67:93–104. https://doi.org/10.1016/j.isprsjprs.2011.11.002

Roloff A, Weisgerber H, Lang U, Stimm B (2008) Enzyklopädie der Holzgewächse. 978-3527-32141-4

Ronch FD, Caudullo G, Tinner W, de Rigo D (2016) *Larix decidua* and other larches in Europe: distribution, habitat, usage and threats

Sauermoser S (1988) Former experiences on the field of afforestations in subalpine regions gained by the forest-technical service of torrent and avalanche control for the last 35 years in Tyrol. International Congress Interpraevent Graz, pp 253–266

Scheidl C, Heiser M, Kamper S, Thaler T, Klebinder K, Nagl F, Lechner V, Markart C, Rammer W, Seidl R (2020a) The influence of climate change and canopy disturbances on landslide susceptibility in headwater catchments. Sci Total Environ 742:140588. https://doi.org/10.1016/j.scitotenv.2020.140588

Scheidl C, Heiser M, Vospernik S, Lauss E, Perzl F, Kofler A, Kleemayr K, Bettella F, Lingua E, Garbarino M, Skudnik M, Trappmann D, Berger F (2020b) Assessing the protective role of alpine forests against rockfall at regional scale. Eur J For Res. https://doi.org/10.1007/s10342-020-01299-z

Scheidl CN, Heiser M, Lechner V, Perzl F, Frank G, Thaler T et al. (2021) Forest stands from high elevation afforestation in the Austrian Alps – past, present and future at a glance. In: Natural hazards in a changing world. 14th Congress INTERPRAEVENT 2021, Bergen, pp 356–364

Schönenberger W, Senn J, Wasem U (1994) Factors affecting establishment of planted trees near timberline. General Technical Report. Whitefish, Montana: USDA, Forest Service

Sebald J, Senf C, Heiser M, Scheidl C, Pflugmacher D, Seidl R (2019) The effects of forest cover and disturbance on torrential hazards: large-scale evidence from the Eastern Alps. Environ Res Lett 14(11):114032. https://doi.org/10.1088/1748-9326/ab4937

Senn J, Schönenberger W (2001) Zwanzig Jahre Versuchsaufforstung Stillberg: Überleben und Wachstum einer subalpinen Aufforstung in Abhängigkeit vom Standort | 20 years experimental afforestation Stillberg: Survival and growth in a subalpine afforestation in relation to site conditions. Schweiz Z Forstwes 152(6):226–246. https://doi.org/10.3188/szf.2001.0226

Sykes J, Haegeli P, Bühler Y (2022) Automated snow avalanche release area delineation in data-sparse, remote, and forested regions. Nat Hazards Earth Syst Sci 22(10):3247–3270. https://doi.org/10.5194/nhess-22-3247-2022

Talukdar S, Eibek KU, Akhter S, Ziaul S, Towfiqul Islam AR, Mallick J (2021) Modeling fragmentation probability of land-use and land-cover using the bagging, random forest and random subspace in the Teesta River Basin, Bangladesh. Ecol Indic 126:107612. https://doi.org/10.1016/j.ecolind.2021.107612

Teich M, Bartelt P, Grêt-Regamey A, Bebi P (2012) Snow avalanches in forested terrain: influence of forest parameters, topography, and avalanche characteristics on runout distance. Arct Antarct Alp Res 44(4):509–519. https://doi.org/10.1657/1938-4246-44.4.509

Teich M, Giunta AD, Hagenmuller P, Bebi P, Schneebeli M, Jenkins MJ (2019) Effects of bark beetle attacks on forest snowpack and avalanche formation: implications for protection forest management. For Ecol Manage. https://doi.org/10.1016/j.foreco.2019.01.052

Amt der Tiroler Landesregierung, Gruppe Forst. (2020) Tiroler Waldbericht 2020 an den Tiroler Landtag über das Jahr 2019. https://www.tirol.gv.at/fileadmin/themen/umwelt/wald/waldzustand/downloads/waldbericht2020.pdf. Accessed 15 June 2022

Amt der Tiroler Landesregierung, Tiris. (2020) Tiroler Rauminformationssystem. https://tiris.maps.arcgis.com/home/index.html. Accessed 15 Sept 2022

Toosi NB, Soffianian AR, Fakheran S, Pourmanafi S, Ginzler C, Waser LT (2019) Comparing different classification algorithms for monitoring mangrove cover changes in southern Iran. Glob Ecol Conserv 19:e00662. https://doi.org/10.1016/j.gecco.2019.e00662

Toscani P (2012) Systematische evaluierung verschiedener datentransformationen für die klassifizierung von wald-, offenland- und Latschen-Flächen in den Bayerischen Alpen. Master thesis. University of Natural Resources and Life Sciences Vienna

Turner H, Häsler R, Schönenberger W (1983) Contrasting microenvironments and their effects on carbon uptake and allocation by young conifers near alpine treeline in Switzerland. In: Wareing RH (ed) Carbon uptake and allocation in subalpine ecosystems as a key to management. IUFRO Workshop 1982, Oregon State University, Forestry Research Laboratory. pp 22–30

Van Herwijnen A, Gaume J, Bair EH, Reuter B, Birkeland KW, Schweizer J (2016) Estimating the effective elastic modulus and specific fracture energy of snowpack layers from field experiments. J Glaciol 62(236):997–1007. https://doi.org/10.1017/jog.2016.90

Waser LT, Ginzler C, Kuechler M, Baltsavias E, Hurni L (2011) Semi-automatic classification of tree species in different forest ecosystems by spectral and geometric variables derived from airborne DIGITAL SENSOR (ADS40) and RC30 data. Rem Sense Environ 115(1):76–85. https://doi.org/10.1016/j.rse.2010.08.006

WIFO (1963) Mehr Holz durch Wiederbewaldung und Neuaufforstung. Austrian Inst Econ Res 1:9–15

Zhang C, Xia K, Feng H, Yang Y, Du X (2021) Tree species classification using deep learning and RGB optical images obtained by an unmanned aerial vehicle. J for Res 32(5):1879–1888. https://doi.org/10.1007/s11676-020-01245-0